Dob1p (Mtr4p) is a putative ATP-dependent RNA helicase required for the 3′ end formation of 5.8S rRNA in *Saccharomyces cerevisiae*

Jesús de la Cruz[1], Dieter Kressler, David Tollervey[2] and Patrick Linder

Département de Biochimie Médicale, Centre Médical Universitaire, Université de Genève, CH-1211 Geneva, Switzerland and [2]Institute of Cell and Molecular Biology, University of Edinburgh, Edinburgh EH9 3JR, UK

[1]Corresponding author
e-mail: Jesus.Cruz@medecine.unige.ch

J.de la Cruz and D.Kressler contributed equally to this work

The temperature-sensitive mutation, *dob1-1*, was identified in a screen for dependence on overexpression of the yeast translation initiation factor eIF4B (Tif3p). Dob1p is an essential putative ATP-dependent RNA helicase. Polysome analyses revealed an under accumulation of 60S ribosomal subunits in the *dob1-1* mutant. Pulse–chase labelling of pre-rRNA showed that this was due to a defect in the synthesis of the 5.8S and 25S rRNAs. Northern and primer extension analyses in the *dob1-1* mutant, or in a strain genetically depleted of Dob1p, revealed a specific inhibition of the 3′ processing of the 5.8S rRNA from its 7S precursor. This processing recently has been attributed to the activity of the exosome, a complex of 3′→5′ exonucleases that includes Rrp4p. *In vivo* depletion of Dob1p also inhibits degradation of the 5′ external transcribed spacer region of the pre-rRNA. A similar phenotype was observed in *rrp4* mutant strains and, moreover, the *dob1-1* and *rrp4-1* mutations show a strong synergistic growth inhibition. We propose that Dob1p functions as a cofactor for the exosome complex that unwinds secondary structures in the pre-rRNA that otherwise block the progression of the 3′→5′ exonucleases.
Keywords: Mtr4p/RNA helicase/rRNA processing/ Rrp4p/*Saccharomyces cerevisiae*

Introduction

In eukaryotes, ribosome biogenesis is a complex process that involves ~80 ribosomal proteins and four mature rRNAs. The mature 60S ribosomal subunit consists of three rRNAs (5S, 5.8S and 28–25S) and ~45 ribosomal proteins, whereas the mature 40S ribosomal subunit is formed by one 18S rRNA molecule and ~35 ribosomal proteins (reviewed in Woolford and Warner, 1991). In all eukaryotes, rRNAs are synthesized as precursors (pre-rRNAs) that require maturation by a large number of non-ribosomal *trans*-acting factors. Transcription of the rDNA, processing and modifications of the pre-rRNAs, and assembly with ribosomal proteins are concomitant processes that take place primarily in a specialized subnuclear compartment termed the nucleolus (reviewed in Mélèse and Xue, 1995). Although ribosome biogenesis has been studied extensively in higher eukaryotes (reviewed in Eichler and Craig, 1994), different biochemical strategies and genetic approaches in the yeast *Saccharomyces cerevisiae* have provided the best characterized picture regarding the various *cis*-elements and *trans*-acting factors participating in this process (reviewed in Lafontaine and Tollervey, 1995; van Nues *et al.*, 1995; Venema and Tollervey, 1995; Tollervey and Kiss, 1997).

In yeast, three of four rRNAs (18S, 5.8S and 25S) are produced as a single 35S precursor by RNA polymerase I, whereas the fourth rRNA (5S) is transcribed independently by RNA polymerase III as a precursor, which is extended at its 3′ end by up to 10 nucleotides (Woolford and Warner, 1991; Venema and Tollervey, 1995). In the 35S pre-rRNA, the mature rRNA sequences are separated by two internal transcribed spacers, ITS1 and ITS2, and flanked by two external transcribed spacers, 5′ ETS and 3′ ETS (see Figure 1A). During the maturation of the 35S pre-rRNA, these transcribed spacers are removed by a series of ordered endo- or exonucleolytic reactions requiring small nucleolar RNAs (snoRNAs) (reviewed in Tollervey and Kiss, 1997) and proteins as *trans*-acting factors (Lafontaine and Tollervey, 1995; Venema and Tollervey, 1995). Concomitantly, the pre-rRNAs are also covalently modified, mostly by 2′-*O*-methylation of ribose groups and conversion of uridine residues to pseudouridine (Tollervey and Kiss, 1997).

The first pre-rRNA processing steps comprise the endonucleolytic cleavages in 5′ ETS and ITS1 at sites A_0, A_1 and A_2 that yield the 20S pre-rRNA, which subsequently is converted into the mature 18S rRNA. Cleavage at site A_2 also gives rise to the $27SA_2$ precursor, which is processed further into the $27SB_L$ and $27SB_S$ species by two alternative pathways in ITS1 (Figure 1B). Final maturation of 5.8S and 25S rRNAs requires ITS2 removal from the 27SB species. In the current model, both the $27SB_L$ and $27SB_S$ molecules follow the same processing pathway (Figure 1B). Processing at sites C_1 and C_2 generates the 5′ end of the mature 25S rRNA and the 3′ end of the $7S_L$ and $7S_S$ pre-rRNAs, the precursors of the mature 5.8S rRNA. Processing of the 7S pre-rRNA to the 5.8S rRNA requires a protein complex, termed the exosome, which includes Rrp4p (Mitchell *et al.*, 1996) and Rrp41p to Rrp44p (Mitchell *et al.*, 1997). Recombinant Rrp4p, Rrp41p and Rrp44p are each 3′→5′ exoribonucleases; Rrp41p is homologous to *Escherichia coli* RNase PH, while Rrp44p is homologous to *E.coli* RNase II. The other components, Rrp42p and Rrp43p, are both members of the RNase PH/PNPase family of ribonucleases, and are therefore also predicted to be 3′→5′ exonucleases (Mian, 1997). The *rrp4-1* mutation or *in vivo* depletion of any component of the exosome results in the accumulation of forms of the 5.8S rRNA that are 3′ extended up to site C_2, the 3′ end of 7S pre-rRNA. Therefore, it has been
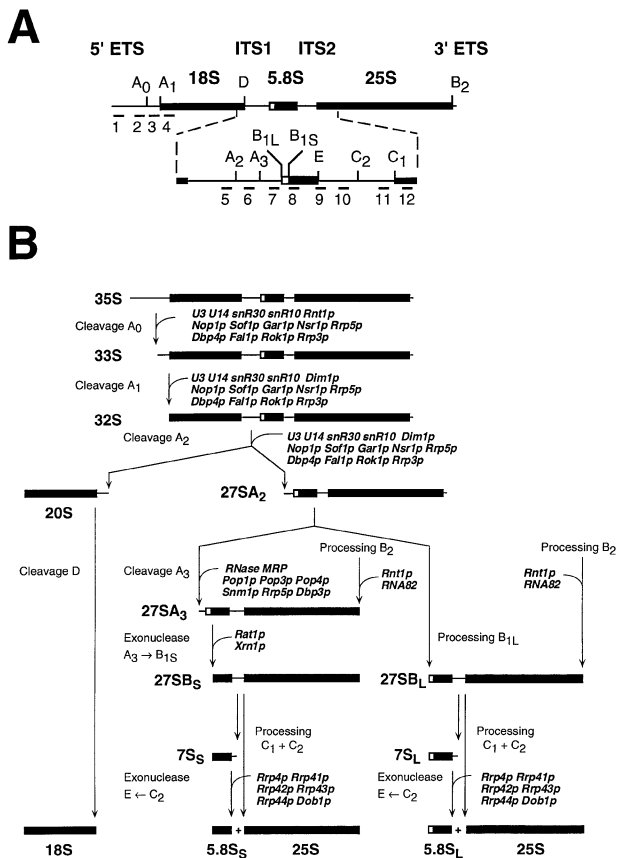
A

5′ ETS   ITS1   ITS2   3′ ETS

A_0 A_1 18S   D   5.8S   25S B_2

1 2 3 4

B_{1L} B_{1S}

A_2 A_3 E C_2 C_1

5   6   7   8   9   10   11 12

B

35S

Cleavage A_0 | *U3 U14 snR30 snR10 Rnt1p*
      Nop1p Sof1p Gar1p Nsr1p Rrp5p
      Dbp4p Fal1p Rok1p Rrp3p

33S

Cleavage A_1 | *U3 U14 snR30 snR10 Dim1p*
      Nop1p Sof1p Gar1p Nsr1p Rrp5p
      Dbp4p Fal1p Rok1p Rrp3p

32S

Cleavage A_2 | *U3 U14 snR30 snR10 Dim1p*
      Nop1p Sof1p Gar1p Nsr1p Rrp5p
      Dbp4p Fal1p Rok1p Rrp3p

$27SA_2$

20S   Processing B_2 Processing B_2

Cleavage D   Cleavage A_3 | *RNase MRP*   *Rnt1p*   *Rnt1p*
      Pop1p Pop3p Pop4p   *RNA82*   *RNA82*
      Snm1p Rrp5p Dbp3p

$27SA_3$

Exonuclease | *Rat1p*   Processing B_{1L}
$A_3 \rightarrow B_{1S}$ *Xrn1p*

$27SB_S$ $27SB_L$

   Processing   Processing
   $C_1 + C_2$ $C_1 + C_2$

     $7S_S$ $7S_L$

Exonuclease | *Rrp4p Rrp41p*   Exonuclease | *Rrp4p Rrp41p*
$E \leftarrow C_2$ *Rrp42p Rrp43p* $E \leftarrow C_2$ *Rrp42p Rrp43p*
      Rrp44p Dob1p   *Rrp44p Dob1p*

18S $5.8S_S$ 25S $5.8S_L$ 25S

Fig. 1. Scheme of 35S pre-rRNA processing in *S.cerevisiae*. (**A**) Structure and processing sites of the 35S pre-rRNA. This precursor contains the sequences for the mature 18S, 5.8S and 25S rRNAs that are separated by the two internal transcribed spacers ITS1 and ITS2. Two external transcribed spacers, the 5′ ETS and the 3′ ETS, are present at either end. The location of various probes (numbered 1–12) used in this study are indicated. Bars represent mature rRNA species and lines the transcribed spacers. (**B**) Pre-rRNA processing pathway. The 35S pre-rRNA is cleaved at site A_0 by the endonuclease Rnt1p, generating the 33S pre-rRNA. This molecule subsequently is processed at sites A_1 and A_2, resulting in the separation of the pre-rRNAs destined for the small and large ribosomal subunits. The early pre-rRNA cleavages A_0 to A_2 are proposed to require a large snoRNP complex, which may be assisted by the putative ATP-dependent RNA helicases Dbp4p, Fal1p, Rok1p and Rrp3p. The final maturation of the 20S precursor takes place in the cytoplasm, where an endonucleolytic cleavage at site D yields the mature 18S rRNA. The $27SA_2$ precursor is processed by two alternative pathways that both lead to the formation of mature 5.8S and 25S rRNAs. In the major pathway, the $27SA_2$ precursor is cleaved at site A_3 by the RNase MRP complex. The putative ATP-dependent RNA helicase Dpb3p assists in this processing step. The $27SA_3$ precursor is exonucleolytically digested 5′→3′ up to site B_{1S} to yield the $27SB_S$ precursor, a reaction requiring the exonucleases Xrn1p and Rat1p. A minor pathway processes the $27SA_2$ molecule at site B_{1L}, producing the $27SB_L$ pre-rRNA. While processing at site B_1 is completed, the 3′ end of mature 25S rRNA is generated by processing at site B_2. The subsequent ITS2 processing of both 27SB species appears to be identical. Cleavage at sites C_1 and C_2 releases the mature 25S rRNA and the 7S pre-rRNA. The latter undergoes exosome-dependent 3′→5′ exonuclease digestion to the 3′ end of the mature 5.8S rRNA. The data presented in this study indicate that Dob1p, a putative ATP-dependent RNA helicase, assists the exosome.

proposed that the 3′ end formation of 5.8S rRNA occurs via a 3′→5′ exonucleolytic processing mechanism (Mitchell *et al.*, 1996, 1997).

In addition to the nucleases, another class of proteins predicted to function enzymatically in ribosome synthesis are the ATP-dependent RNA helicases. To date, eight putative RNA helicases have been reported to be required for normal pre-rRNA processing in yeast; Dbp4p, Fal1p, Rok1p and Rrp3p are required for 18S rRNA synthesis (O'Day *et al.*, 1996; Kressler *et al.*, 1997; Liang *et al.*, 1997; Venema *et al.*, 1997a), while Dbp3p, Dbp6p, Drs1p and Spb4p are involved in the maturation of the 25S and 5.8S rRNAs (Sachs and Davis, 1990; Ripmaster *et al.*, 1992; Weaver *et al.*, 1997; D.Kressler, J.de la Cruz, M.Rojo and P.Linder, in preparation). RNA unwinding activities might be required to provide access to the pre-rRNA at sites of an endonucleolytic cleavage, as has been suggested for Dbp3p and Fal1p (Kressler *et al.*, 1997; Weaver *et al.*, 1997), or they could open secondary structures in pre-rRNA substrates that might otherwise stall or block the activity of exonucleases. In addition, many snoRNAs form extensive base-paired interactions with the pre-rRNAs (Tollervey and Kiss, 1997). Thus, it is likely that RNA helicases play roles in the association/dissociation reactions of these snoRNAs with the pre-rRNA, as has been suggested for Dbp4p and Rok1p (Liang *et al.*, 1997; Venema *et al.*, 1997a). Finally, extensive structural rearrangements of the pre-rRNAs and the ribosomal proteins are expected to occur during the assembly reactions, and these are likely to require RNA helicases. This may be the function of Drs1p, Dbp6p and Spb4p (Sachs and Davis, 1990; Ripmaster *et al.*, 1992; D.Kressler, J.de la Cruz, M.Rojo and P.Linder, in preparation).

In a genetic screen for mutants dependent on overexpression of Tif3p, the yeast homologue of the mammalian translation initiation factor eIF4B (Altmann *et al.*, 1993; Coppolecchia *et al.*, 1993), we isolated *dob1-1* (<u>d</u>ependent <u>o</u>n eIF4<u>B</u>). Nucleotide sequence and disruption analyses indicated that *DOB1* encodes an essential member of a subfamily of putative RNA helicases that includes Ski2p (Widner and Wickner, 1993). During the progress of this work, *DOB1* was identified independently as *mtr4-1*, a mutation leading to nuclear poly(A)+ RNA accumulation (Liang *et al.*, 1996). Analysis of the *dob1-1* mutant and a Dob1p-depleted strain demonstrates that Dob1p functionally interacts with the exosome complex during pre-rRNA processing.

Results

Isolation of the dob1-1 mutant as a TIF3 multicopy-dependent mutation

We have carried out a screen to isolate mutants that are dependent on a high copy number of the *TIF3* gene. For this purpose, an *ade2/ura3* strain (CW04, Table I) was transformed with pDK17-TIF3, a 2μ-*ADE2/URA3* plasmid bearing a wild-type *TIF3* gene. The resulting strain MS04 is white, but loss of pDK17-TIF3 results in red colonies. Thus, growth of MS04 on non-selective medium leads to white/red sectoring colonies. This strain was mutagenized by treatment with ethylmethane sulfonate (EMS) at a dose giving a ~70% survival rate, and cells were plated out on rich, non-selective medium (YPD). Among 15 000 surviving colonies, 31 were completely white. These colonies were restreaked twice for single colonies on YPD plates, and white, non-sectoring candidates were tested for growth on plates containing 5-fluoro-orotic acid (5-FOA). Cells carrying a functional *URA3* gene are sensitive to

Table I. Yeast strains used in this study

Name	Genotype	Reference/source
CW04	*MATα, ura3-1, ade2-1, his3-11,15, leu2-3,112, trp1-1*	Banroques *et al.* (1986)
ASZ1	*MATa, ura3-1, ade2-1, his3-11,15, leu2-3,112, trp1-1*	Coppolecchia *et al.* (1993)
ASZ3	*MATα/MATa, ura3-1/ura3-1, ade2-1/ade2-1, his3-11,15/his3-11,15, leu2-3,112/leu2-3,112, trp1-1/trp1-1*	Coppolecchia *et al.* (1993)
MS04	*MATα, ura3-1, ade2-1, his3-11,15, leu2-3,112, trp1-1* [pDK17-TIF3]	this work
MS157	*MATα, ura3-1, ade2-1, his3-11,15, leu2-3,112, trp1-1, dob1-1* [pDK17-TIF3]	this work
MS157-1A	*MATa, ura3-1, ade2-1, his3-11,15 , leu2-3,112, trp1-1, dob1-1*	this work
JDY1	*MATα/MATa, ura3-1/ura3-1, ade2-1/ade2-1, his3-11,15/his3-11,15, leu2–3,112/leu2-3,112, trp1-1/trp1-1, DOB1/dob1::HIS3MX6*	this work
JDY3[a]	*MATα, ura3-1, ade2-1, his3-11,15, leu2-3,112, trp1-1, dob1::HIS3MX6* [YCplac33-DOB1]	this work
D150	*MATa, ura3-52, ade1-100, his4-519, leu2-3,112*	P.Mitchell (Edinburgh, UK)
P54	*MATa, ura3-52, ade1-100, his4-519, leu2-3,112, rrp4-1*	P.Mitchell (Edinburgh, UK)
P79	*MATa, ura3-52, ade1-100, his4-519, leu2-3,112, GAL::RRP4*	P.Mitchell (Edinburgh, UK)
P47	*MATα/MATa, ura3-52/ura3-52, ade2-1/ade2-1, his3-11,15/his3-11,15, leu2–3,112/leu2-3,112, trp1-1/trp1-1, GAL::RRP4/rrp4::HIS3*	P.Mitchell (Edinburgh, UK)
D184	*MATa, ura3-52, ade2-1, his3-11,15, leu2-3,112, trp1-1, xrn1::URA3*	B.Dichtl (Edinburgh, UK)
966-1C	*MATa, ura3-52, xrn1::URA3, rat1-1*	B.Dichtl (Edinburgh, UK)
JDY4	*MATα, ura3-52, ade2-1, his3-11,15, leu2-3,112, trp1-1, rrp4::HIS3* [pRS415-rrp4-1]	this work
JDY5	*MATa, ura3-52, ade2-1, his3-11,15, leu2–3,112, trp1-1, rrp4::HIS3* [pRS416-ProtA-RRP4]	this work
JDY6	*MATα/MATa, ura3-1/ura3-52, ade2-1/ade2-1, his3-11,15/his3-11,15, leu2–3,112/leu2-3,112, trp1-1/trp1-1, DOB1/dob1::HIS3MX6, RRP4/rrp4::HIS3* [YCplac111-HA-DOB1, pRS416-ProtA-RRP4]	this work
JDY7	*MATα, ura3, ade2-1, his3-11,15, leu2-3,112, trp1-1, dob1::HIS3MX6, rrp4::HIS3* [YCplac111-HA-DOB1, pRS416-ProtA-RRP4]	this work

[a]Depending on the experimental conditions, the original YCplac33-DOB1 was replaced by other *DOB1*-containing plasmids.

5-FOA, therefore mutants unable to lose pDK17-TIF3 should not grow on that medium. Four such mutants were identified and transformed with a *CEN-LEU2* vector (YCplac111), a 2μ-*LEU2* vector (YEplac181) and their respective constructs carrying *TIF3*. One mutant, MS157, regained red sectoring and 5-FOA resistance when transformed with YEplac181-TIF3 but not with YEplac181 or YCplac111-TIF3, demonstrating that MS157 carries a *TIF3* multicopy-dependent mutation that was designated *dob1-1*. In addition, MS157 showed a slow growth phenotype at 30°C and did not grow at 37°C. Furthermore, MS157 was sensitive to the aminoglycoside paromomycin, an inhibitor of translation, to the same extent as mutants affected in translation initiation factors (*tif1-1*, *Δtif3*, *Δtif4631*, *cdc33-1*, *cdc33-42*, *prt1-1*; de la Cruz *et al.*, 1997) (data not shown).

To eliminate undesired second site mutations, MS157 was back-crossed to an isogenic wild-type strain (ASZ1). The heterozygous *dob1-1/DOB1* diploid was neither temperature-sensitive (ts) nor sensitive to paromomycin, indicating that *dob1-1* is recessive. After analysis of 20 complete tetrads of the *dob1-1/DOB1* strain, the ts and the drug sensitivity phenotypes segregated $2^+:2^-$ and co-segregated with each other, indicating that both phenotypes were due to a single nuclear mutation. A ts and drug-sensitive haploid strain (MS157-1A, Table I), derived from three consecutive crosses with ASZ1, was used to confirm the *dob1-1* phenotype. As shown in Figure 2, the growth of MS157-1A was not strictly dependent on a 2μ construct harbouring *TIF3* at 30°C; however, the ts phenotype was partially suppressed at 35°C by the multicopy *TIF3* plasmid. This suppression was *TIF3* specific, since multicopy plasmids bearing genes encoding other yeast translation initiation factors (eIF4A, eIF4E and eIF4G₁) were not able to confer suppression (data not shown). Finally, quantitative Western blot analyses showed identical Dob1p levels in the wild-type (MS04 and CW04) and the *dob1-1*

mutant (MS157-1A) strains, either at permissive temperature or 12 h after a shift to 37°C (data not shown).

DOB1 encodes an essential putative ATP-dependent RNA helicase

To isolate the *DOB1* gene, MS157-1A was transformed with a YCplac111-based yeast genomic library and screened for growth at 37°C. Two independent clones (pDK102 and pDK103) that reproducibly complemented the ts phenotype were recovered (Figure 2). The flanking sequences of these clones were determined and compared with the yeast genome database. Both clones contained DNA from chromosome X and shared a 6 kb fragment. Subcloning defined the minimal region required for complementation as a 4 kb fragment containing a unique open reading frame (ORF) of 3219 nucleotides (YJL050W), which encodes a protein of 1073 amino acids with a predicted molecular mass of 122 kDa. Comparison of the deduced amino acid sequence with databases revealed that Dob1p belongs to a subfamily of putative ATP-dependent RNA helicases, which includes the yeast Ski2p (37% identity over their entire lengths; Widner and Wickner, 1993) and, as the most related proteins, the predicted product from human (52% identity; Dangel *et al.*, 1995), *Drosophila melanogaster* (49% identity; GenBank accession No. Ac000510) and *Caenorhabditis elegans* (44% identity; GenBank accession No. Z70271) cDNA clones. This strong sequence conservation between these distant eukaryotes suggests that the function of Dob1p is evolutionarily conserved.

To analyse the *in vivo* function of *DOB1*, we replaced almost the entire ORF by a HIS3MX6 cassette (see Materials and methods). The *dob1*::HIS3MX6 construct was integrated at the *DOB1* genomic locus in the diploid strain ASZ3 to generate the strain JDY1. Correct gene replacement was verified by Southern blot analysis. Analysis of 20 complete tetrads showed a 2:2 segregation of
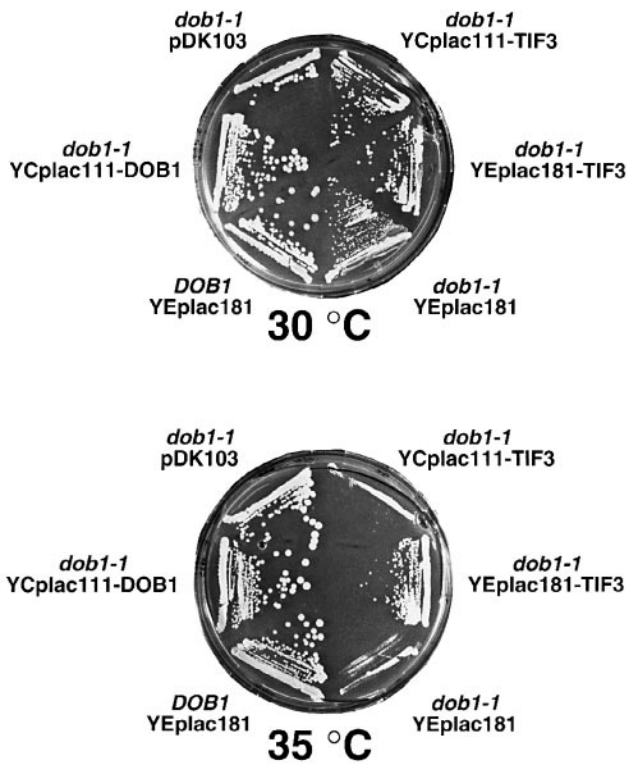
Fig. 2. The *dob1-1* mutant is dependent on a high dosage of *TIF3*. The strain MS157-1A (*dob1-1*) was transformed with either YEplac181 (2μ), YEplac181-TIF3 (2μ-*TIF3*), YCplac111-TIF3 (*CEN-TIF3*) or the complementing plasmids pDK103 (*CEN-DOB1*) and YCplac111-DOB1, a subclone of pDK102 (*CEN-DOB1*). As a control, the isogenic wild-type strain CW04 (*DOB1*) was transformed with YEplac181. Transformants were grown on SD-Leu plates at 30 or 35°C for 4 days.

viable to non-viable spores, with all the viable progeny being auxotrophic for histidine and, therefore, Dob1+. When JDY1 was transformed with YCplac33-DOB1 and subsequently sporulated, complete tetrads could germinate and grow. All the haploid *dob1*::HIS3MX6 progeny (His+) contained the YCplac33-DOB1 plasmid (Ura+) and were unable to grow on plates containing 5-FOA (data not shown). These results demonstrated that Dob1p is essential for cell viability.

To determine whether the plasmid that complemented the *dob1-1* mutation contained the *DOB1* gene rather than a low copy number suppressor, MS157-1A was crossed with JDY3 YCplac33-DOB1 (a *dob1*::HIS3MX6 strain containing a wild-type copy of *DOB1* in a *CEN-URA3* plasmid). After sporulation and tetrad dissection, a 2 His+:2 His− segregation was obtained. Twenty complete tetrads were tested by selection against the plasmid on plates containing 5-FOA; two viable ts and His−-spore clones were recovered in each case. These results indicated that the gene complementing the *dob1-1* mutation is genetically linked to the *DOB1* locus.

During the progress of this work, *DOB1* was identified in a screen for mutants that accumulate nuclear poly(A)+ RNA and was designated *MTR4* (Liang *et al.*, 1996).

Construction of a GAL::DOB1 strain
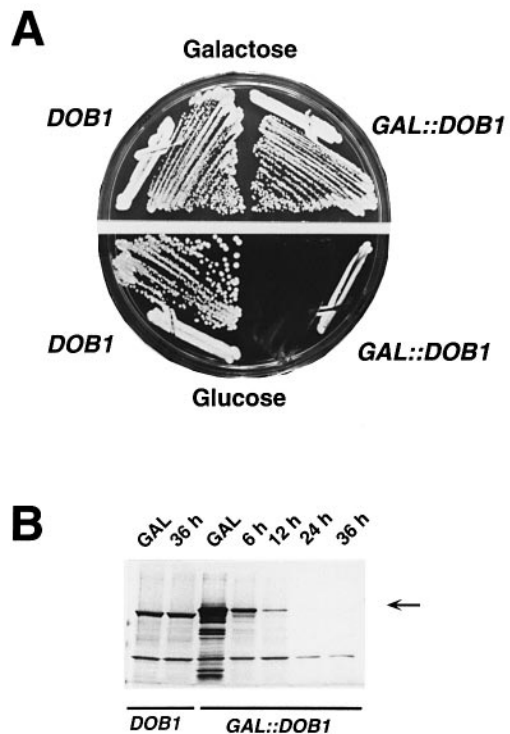To study better the function of Dob1p, a different conditional system for phenotypic analysis was established.

Fig. 3. *In vivo* depletion of Dob1p. (**A**) Growth comparison of JDY3 pAS24-DOB1 (*GAL::DOB1*) and its isogenic counterpart JDY3 YCplac111-DOB1 (*DOB1*). Cells were streaked on YPGal (galactose) or YPD (glucose) plates and incubated for 4 days at 30°C. (**B**) Detection of Dob1p by Western blotting. The strains JDY3 YCplac111-DOB1 (*DOB1*) and JDY3 pAS24-DOB1 (*GAL::DOB1*) were grown in YPGal and shifted to YPD for up to 36 h. Cell extracts were prepared from samples harvested at the indicated times and assayed by Western blotting. Equal amounts of total protein (70 μg) were loaded in each lane, as judged by Coomassie staining of gels or red Ponceau staining of the blots (data not shown). Polyclonal rabbit anti-Dob1p antibodies followed by alkaline phosphatase-coupled goat anti-rabbit IgG were used to detect Dob1p. The Dob1p signal is indicated by an arrow. Note the differences in mobility between Dob1p and HA-Dob1p, due to the N-terminal translational fusion of a double HA tag. Note also that a cross-reacting band (~70 kDa) is not depleted upon growth of JDY3 pAS24-DOB1 in YPD.

To this end, the *DOB1* ORF was cloned into pAS24 under the control of a hybrid *GAL1-10* promoter, which allows expression in medium containing galactose but is repressed in glucose-based medium. The plasmid pAS24-DOB1 fully complemented the *dob1* null (JDY3) on YPGal but resulted in impaired growth on YPD plates (Figure 3A). Reproducibly, after shifting a mid-logarithmic culture of JDY3 pAS24-DOB1 from liquid YPGal medium to YPD medium, the growth rate decreased progressively to a doubling time of >10 h after 24 h in YPD, as compared with the 2 h doubling time for the isogenic control strain JDY3 YCplac111-DOB1. A concomitant depletion of Dob1p was observed by Western blotting, also as compared with JDY3 YCplac111-DOB1 (Figure 3B).

The dob1-1 and GAL::DOB1 strains are deficient in 60S ribosomal subunits
The suppression by high dosage of *TIF3* and the sensitivity to paromomycin suggested that the *dob1-1* mutation impaired protein synthesis. To test this hypothesis, we performed polysome profile analyses. At 30°C, when
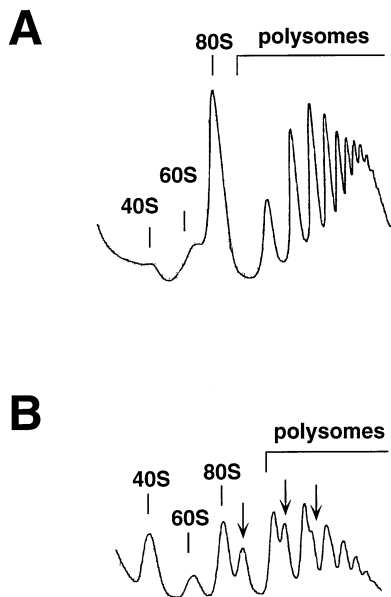
A

B

Fig. 4. The *dob1-1* mutation results in a deficit of free 60S ribosomal subunits and in the accumulation of half-mer polysomes. (**A**) CW04 (*DOB1*); (**B**) MS157-1A (*dob1-1*). Cells were grown at 30°C, harvested at an $OD_{600\,nm}$ of 0.8, and cell extracts were resolved in 7–50% sucrose gradients. The $A_{254\,nm}$ was measured continuously. Sedimentation is from left to right. The peaks of free 40S and 60S ribosomal subunits, 80S free couples/monosomes and polysomes are indicated. Half-mers are labelled by vertical arrows.

compared with wild-type cells (Figure 4A), the *dob1-1* mutant showed a deficit of free 60S relative to free 40S ribosomal subunits, an overall decrease in 80S ribosomes (free couples and monosomes) and polysomes, and an accumulation of half-mer polysomes (Figure 4B). These features were even more pronounced when *dob1-1* cells were shifted to 37°C for 12 h (data not shown). Complementation of *dob1-1* by a *CEN* plasmid containing *DOB1* resulted in wild-type polysome profiles (data not shown). The presence of half-mer polysomes is indicative of a defect in a late step of the translation initiation pathway (Foiani *et al.*, 1991; Kang and Hershey, 1994) or the result of a reduction in the number of 60S ribosomal subunits due to mutations either in proteins of the 60S ribosomal subunit (Moritz *et al.*, 1991; Deshmukh *et al.*, 1993; Vilardell and Warner, 1997), or in components involved in pre-rRNA processing and 60S ribosomal subunit assembly (Ripmaster *et al.*, 1992; Hong *et al.*, 1997; Weaver *et al.*, 1997). To distinguish between a role for Dob1p in translation initiation or in 60S ribosomal subunit biogenesis, the relative amounts of total 40S and 60S ribosomal subunits were quantified. An $A_{254\,nm}$ 60S/40S ratio of ~1.5 was obtained for the *dob1-1* mutant, while this ratio was ~2 for the isogenic wild-type strain or for the *dob1-1* mutant complemented with a *CEN-DOB1* plasmid.

When polysomes were analysed from the *GAL::DOB1* strain following transfer to YPD medium, an overall decrease in polysomes and a slight appearance of half-mer polysomes were observed during depletion of Dob1p (data not shown). Quantification of total ribosomal subunits showed a 60S to 40S ribosomal subunit imbalance, which lowered the $A_{254\,nm}$ 60S/40S ratio to ~1.7 after 36 h of depletion. These results indicated that the *dob1-1* mutation

and the *in vivo* depletion of Dob1p both lead to similar deficiencies in the 60S ribosomal subunit synthesis.

Furthermore, Western blot analyses on ribosomal subunits purified after sucrose gradient fractionation failed to detect Dob1p (data not shown). In addition, we and others have immunolocalized an N-terminally HA-tagged Dob1p in the nucleus (Liang *et al.*, 1996, and data not shown).

Taking all these results together, we conclude that Dob1p is not a structural component of the 60S ribosomal subunit but is required for its normal biogenesis.

The dob1-1 mutation impairs pre-rRNA processing

To determine whether Dob1p is required for synthesis or processing of pre-rRNAs, *dob1-1* (MS157-1A) and *DOB1* (CW04) cells were labelled *in vivo* with [methyl-^{3}H]-methionine at 30°C for 3 and 6 min, and chased with an excess of cold methionine for 5 or 15 min. Total RNA was extracted and samples were analysed by agarose gel electrophoresis, followed by transfer to a Nylon filter and fluorography. In wild-type cells, the 35S and 32S precursors, the 27SA and 27SB pre-rRNAs and the 20S pre-rRNA were detected within the first 3 min of the pulse (Figure 5A, lane 1). After 5 min of the chase, the majority of label was in the mature 25S and 18S rRNAs (Figure 5A, lane 3). In contrast, pre-rRNA processing was slowed in *dob1-1* cells (Figure 5A, lanes 5–8). The 27S species persisted after 15 min of the chase, and a lower yield of labelled 25S rRNA was detected. In contrast, 18S rRNA was produced from its 20S precursor with kinetics and yield similar to wild-type cells (Figure 5A, lanes 4 and 8).

To exclude a defect in methylation and to monitor the processing and synthesis of small RNAs, MS157-1A and CW04 were also labelled *in vivo* with [5,6-^{3}H]uracil for 3 and 6 min, and then chased with an excess of cold uracil for 5, 10 and 30 min. The analysis of high molecular weight RNAs by agarose gel electrophoresis gave similar results to those seen with labelled methyl-methionine (data not shown). Low molecular weight RNA species were analysed by polyacrylamide gel electrophoresis (Figure 5B). Labelling of tRNAs and 5S rRNA were comparable in both kinetics and levels in wild-type and *dob1-1* cells. However, the synthesis of mature 5.8S rRNA was substantially delayed in *dob1-1* cells, and a marked accumulation of a species with the gel mobility of the 7S pre-rRNA was observed (Figure 5B, lanes 8–10).

Thus, the deficit in 60S ribosomal subunit observed in the *dob1-1* strain is a consequence of impaired pre-rRNA processing, leading to a reduced synthesis of both the mature 25S and 5.8S rRNAs.

Dob1p is required for normal pre-rRNA processing

To define the pre-rRNA processing steps that are affected after mutation in or *in vivo* depletion of Dob1p, steady-state levels of mature rRNA and pre-rRNA intermediates were also assessed by Northern and primer extension analyses. Northern analyses of high molecular weight RNAs confirmed the results of the pulse–chase labelling experiments (Figure 6). The levels of mature 25S rRNA were slightly reduced in the *dob1-1* mutant strain (Figure 6A, lanes 2 and 4). The 35S pre-rRNA (Figure 6B–G, lanes 2 and 4) and the aberrant 23S pre-RNA species, which extends from the 5′ end of the 35S pre-rRNA to site A_3 in ITS1, accumulated (Figure 6B–D, lanes 2 and
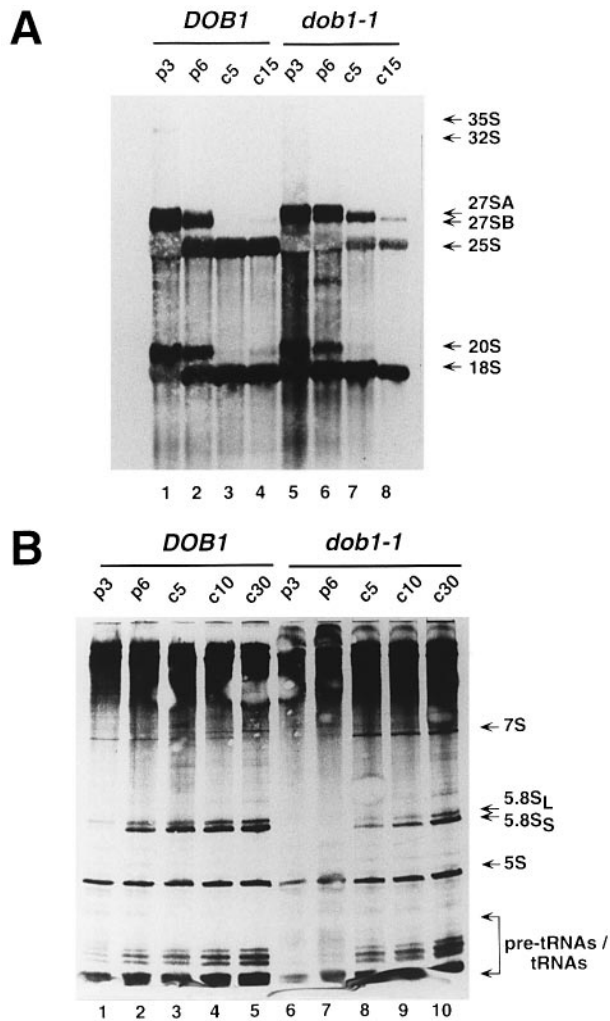
Fig. 5. The *dob1-1* mutation results in reduced synthesis of 25S and 5.8S rRNAs. (**A**) Strains CW04 (*DOB1*) and MS157-1A (*dob1-1*) were grown in YPD, transferred to SD medium lacking methionine, pulse-labelled with [methyl-^{3}H]methionine for 3 and 6 min, and then chased with an excess of cold methionine for 5 and 15 min. (**B**) Strains CW04 (*DOB1*) and MS157-1A (*dob1-1*) were grown in YPD, transferred to SD medium lacking uracil, pulse-labelled with [5,6-^{3}H]uracil for 3 and 6 min, and then chased with an excess of cold uracil for 5, 10 and 30 min. Total RNA was extracted, separated on 1.2% agarose–formaldehyde (A) or 7% polyacrylamide–8 M urea gels (B), transferred to a Nylon membrane and visualized by fluorography. Approximately 20 000 c.p.m. were loaded in each lane. The positions of the different pre-rRNAs and mature rRNAs and tRNAs are indicated.

4). However, the levels of the 20S pre-rRNA and the mature 18S rRNA were not clearly affected (Figure 6A and C). In the *GAL::DOB1* strain depleted of Dob1p by growth on glucose medium, the 23S was observed, together with the 22S and 21S pre-RNA species that extend from sites A_0 and A_1, respectively, to site A_3 (data not shown). As in the *dob1-1* strain, the levels of the 20S pre-rRNA and 18S rRNA were little altered, while the 25S rRNA was depleted (data not shown).

In many mutant strains, accumulation of the 35S pre-rRNA and the aberrant 23S species is associated with the loss of the 20S pre-rRNA, and therefore of the mature 18S rRNA (Venema and Tollervey, 1995). This, however, is not the case in the *dob1*-mutant strains, indicating that the cleavages at sites A_0, A_1 and A_2 are only kinetically

delayed. Interestingly, several other mutants that are defective in the synthesis of the 25S/5.8S rRNAs, i.e. *dbp3*, *nip7*, *nop2*, *nop4/nop77* and *rrp4* (Bergès *et al.*, 1994; Sun and Woolford, 1994; Mitchell *et al.*, 1996; Weaver *et al.*, 1997; Zanchin *et al.*, 1997), also show an accumulation of the 35S pre-rRNA and 23S RNA without depletion of the 20S pre-rRNA or 18S rRNA. We conclude that a mild kinetic delay of processing at sites A_0, A_1 and A_2, rather than a block to processing at these sites, is a distinctive characteristic of mutations interfering with 25S/5.8S rRNA synthesis. The mechanism involved is unclear, although some form of negative feedback on the processing machinery responsible for these cleavages is a possibility.

Analysis of low molecular weight RNA showed a strong accumulation of a pre-rRNA species of ~300 nucleotides in the *dob1-1* strain at 30 or 37°C (Figure 7A and B, lanes 2 and 4). This species hybridized with probes in the 5′ region of ITS2 between sites E and C_2 (probe 10, Figure 7B; probe 9, data not shown), failed to hybridize with probe 11 in the 3′ region of ITS2 or with probe 7 in the 3′ region of ITS1 (data not shown) and had the same mobility as the 7S pre-rRNA of wild-type cells (Figure 7B). We conclude that the *dob1-1* strain strongly accumulates the full-length 7S pre-rRNA. The increase in the 7S pre-rRNA levels was accompanied by a slight depletion of the mature $5.8S_L$ and $5.8S_S$ rRNAs (Figure 7A, lanes 2 and 4). A dramatic accumulation of the 7S pre-rRNA was also seen in the *GAL::DOB1* strain upon depletion of Dob1p (Figure 7B, lanes 7–11) and, in consequence, the steady-state levels of the mature $5.8S_L$ and $5.8S_S$ rRNAs decreased (Figure 7A, lanes 7–11). Northern analysis using probe 13, which hybridizes to sequences in the 5S rRNA, did not reveal any alteration in 5S rRNA synthesis or processing either in the *dob1-1* mutant or after depletion of Dob1p (data not shown).

Primer extension analyses on RNA from the *dob1-1* and Dob1p-depleted strain confirmed the decrease in the steady-state levels of $5.8S_L$ and $5.8S_S$ rRNAs, as shown by the stops at sites B_{1L} and B_{1S} when probe 8 was used as a primer (Figure 7C, lanes 2, 4 and 7–11). Stops at these sites were correct at the nucleotide level, as compared with the isogenic wild-type strain, indicating that the 5′ end of 5.8S rRNA was processed normally in the *dob1*-mutant strains. Increases in the primer extension stops at both B_{1L} and B_{1S} sites were observed when using a probe that hybridizes to the 7S pre-rRNA (probe 10; data not shown). Thus, these data indicated that both the $7S_L$ and $7S_S$ pre-rRNAs accumulated in the *dob1-1* and the Dob1p-depleted strain.

Together, these results indicate that the *dob1-1* mutation and the *in vivo* depletion of Dob1p specifically inhibit the 3′ processing of the $7S_L$ and $7S_S$ pre-rRNAs, resulting in the accumulation of these precursors and a reduced synthesis of the mature $5.8S_L$ and $5.8S_S$ rRNAs. The 5.8S and 25S rRNAs, which are both components of the 60S ribosomal subunit, can only be utilized in a 1:1 ratio (Woolford and Warner, 1991). A reduction in the synthesis of the 5.8S rRNA may therefore also be responsible for the reduced accumulation of the 25S rRNA.

Interestingly, another small rRNA species accumulated strongly after depletion of Dob1p. This species hybridized only with probes 5′ to site A_0 in the 5′ ETS region (Figure 8A and B, lane 6), and migrated on polyacrylamide gels
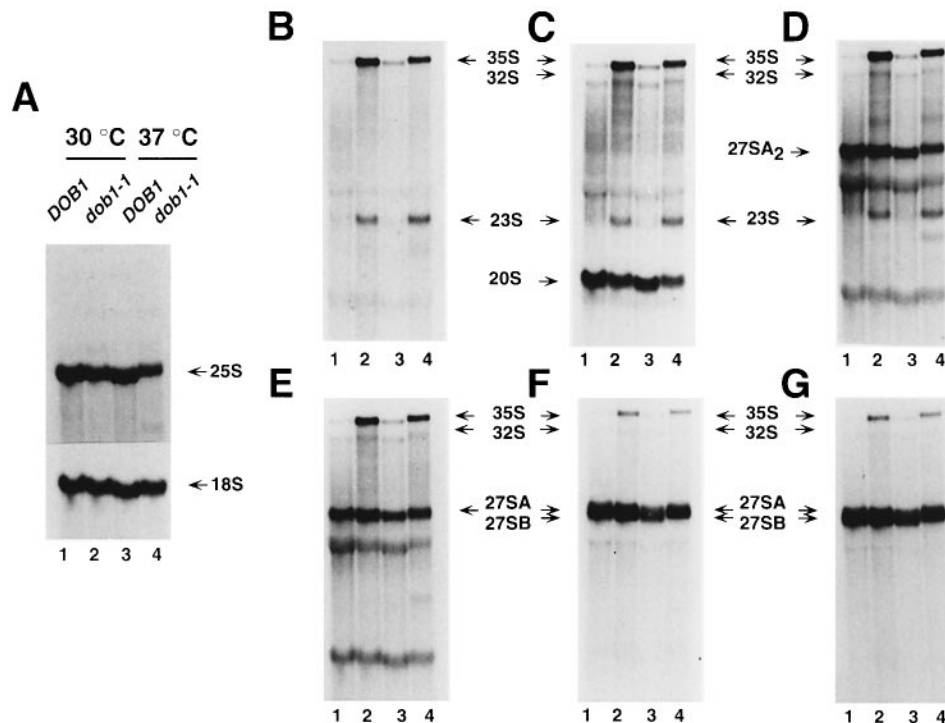
Fig. 6. Effects of the *dob1-1* mutation on steady-state levels of pre-rRNA and mature rRNA species. RNA was extracted from wild-type CW04 (*DOB1*) and MS157-1A (*dob1-1*) cells following growth in YPD at 30°C or 12 h after a shift to 37°C. Equal amounts of total RNA were resolved on a 1.2% agarose–formaldehyde gel and transferred to a Nylon membrane for Northern hybridization. The same filter was hybridized consecutively with all of the different probes used. (**A**) Hybridization with probes 4 and 12 (see Figure 1A for location of the probes), base pairing to sequences within the mature 18S and 25S rRNAs, respectively; (**B**) probe 2 in the 5′ ETS; (**C**) probe 5 in ITS1, between sites D and A_2; (**D**) probe 6 in ITS1, between sites A_2 and A_3; (**E**) probe 7, 3′ to site A_3; (**F**) probe 10 in ITS2, between sites E and C_2; (**G**) probe 11 in ITS2, between sites C_2 and C_1. The positions of the different pre-rRNAs and mature rRNAs are indicated by arrows.

as a single band of approximately the same mobility as the snoRNA snR30 (~610 nucleotides). This species is likely to extend from the 5′ end of the 35S pre-rRNA to site A_0 and was designated 5′-A_0. We conclude that the strain depleted of Dob1p, but not the *dob1-1* mutant, is defective in the degradation of the pre-rRNA spacer fragment generated by cleavage of the 35S pre-rRNA at site A_0. The detection of this fragment also indicates that processing at site A_0 is generated by an endonucleolytic cleavage. We assume that the *dob1-1* mutation shows incomplete penetrance for this phenotype.

Dob1p functionally interacts with Rrp4p

The defective 5.8S rRNA maturation observed in the *dob1-1* and the *GAL::DOB1* strains resembles the phenotypes described for the *rrp4-1* mutant (Mitchell *et al.*, 1996) and strains genetically depleted of Rrp4p, Rrp41p, Rrp42p, Rrp43p or Rrp44p (Mitchell *et al.*, 1997). These strains accumulate heterogeneous 3′-extended forms of 5.8S rRNA, which extend to the 3′ end of the 7S pre-rRNA (Figure 8C, lanes 7–11) accompanied by depletion of the 5.8S (Figure 8D, lanes 7–11) and 25S rRNAs, and they also accumulate the aberrant 23S, 22S and 21S species (Mitchell *et al.*, 1996, 1997).

To determine whether the similarities in phenotypes extend to the defect in degradation of the 5′-A_0 spacer fragment, RNA from *rrp4-1* and *GAL::RRP4* strains was analysed by Northern hybridization using probe 2 (Figure 1A) which hybridizes to the pre-rRNA immediately 5′ to site A_0. Under non-permissive conditions, both strains clearly accumulated the 5′-A_0 spacer fragment (Figure

7A, lanes 7–11). Further analyses demonstrated that the 5′-A_0 fragment is also accumulated after *in vivo* depletion of Rrp41p, Rrp42p, Rrp43p or Rrp44p (data not shown). When a probe that hybridizes closer to site +1 was used (probe 1; Figure 1A), heterogeneous species with sizes extending up to the 5′-A_0 fragment were detected in the *rrp4* mutant strains, but not in the strain depleted of Dob1p (Figure 8B, lanes 6, 9 and 11). It is very likely that these bands correspond to partially degraded 5′-A_0 fragment molecules. Neither the entire 5′-A_0 fragment nor partially degraded forms were detectable in strains carrying mutations in the 5′→3′ exonucleases Xrn1p and Rat1p (Figure 8A and B, lanes 12–13). These two 5′→3′ exonucleases are required for the 5′ end maturation of 5.8S$_S$ rRNA (Henry *et al.*, 1994) and for the degradation of several excised pre-rRNA spacer fragments, the A_0–A_1, D–A_2 and A_2–A_3 regions (Stevens *et al.*, 1991; E.Petfalski, T.Dandekar, Y.Henry and D.Tollervey, in preparation).

These results indicated that the turnover of the 5′-A_0 pre-rRNA also occurs via a 3′→5′ exonucleolytic mechanism that requires both the exosome complex and Dob1p. Heterogeneous populations of 3′-extended forms of the 5.8S rRNA and degradation intermediates of the 5′-A_0 fragment are observed in mutants affecting the exosome components, but not in the Dob1p-depleted strain. This indicated that these RNAs can be partially processed or degraded in the absence of a complete, functional exosome complex but not after the loss of Dob1p function.

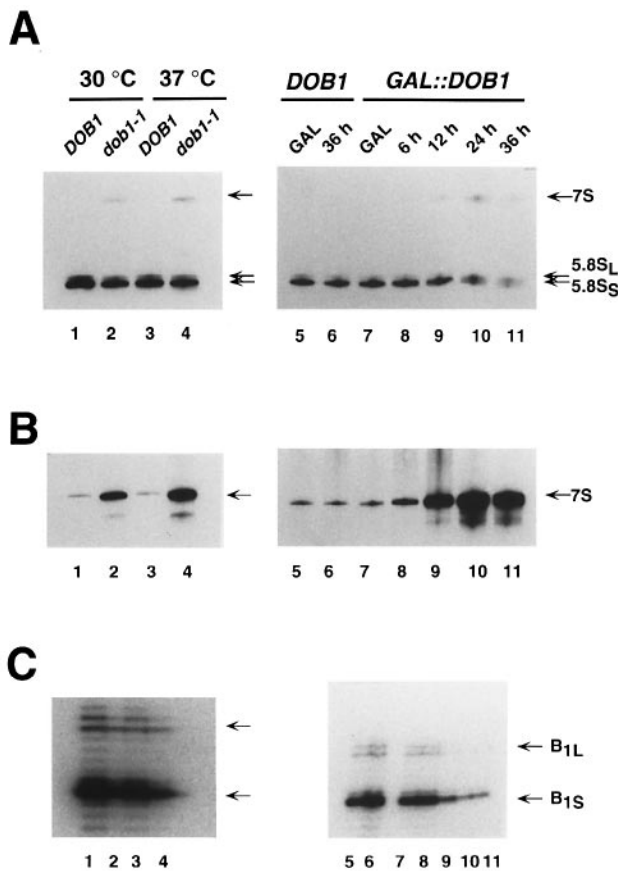Genetic interactions were also analysed between Dob1p and Rrp4p. The growth of a strain carrying both the

Fig. 7. The *dob1-1* mutation and *in vivo* depletion of Dob1p inhibits the 3′ end maturation of 5.8S rRNA. RNA was extracted from wild-type CW04 (*DOB1*) and MS157-1A (*dob1-1*) cells following growth in YPD at 30°C or 12 h after a shift to 37°C. The strains JDY3 YCplac111-DOB1 (*DOB1*) and JDY3 pAS24-DOB1 (*GAL::DOB1*) were grown in YPGal and shifted to YPD for up to 36 h, and RNA was extracted from samples harvested at the indicated times. Equal amounts of total RNA were resolved on a 7% polyacrylamide–8 M urea gel and transferred to a Nylon membrane for Northern hybridization (A and B) or subjected to primer extension analysis (C). (**A**) Hybridization with probe 8 (see Figure 1A for location of the probes), complementary to sequences within the mature 5.8S rRNA species. (**B**) Hybridization with probe 10, base pairing to sequences within the 5′ ITS2 region. (**C**) Primer extension analysis through the processing sites B_{1S} and B_{1L} using oligonucleotide 8. Arrows indicate the positions of the different pre-rRNAs and mature rRNAs, as well as the primer extension stops corresponding to the different pre- and mature rRNA species analysed.

Fig. 8. Comparison of the steady-state levels of the $5'-A_0$ fragment, 7S pre-rRNA and mature 5.8S rRNA in Dob1p, Rrp4p and Xrn1p Rat1p affected strains. Yeast strains were grown in YPD as follows: lanes 1 and 2, CW04 (*DOB1*) and MS157-1A (*dob1-1*) at 30°C; lanes 3 and 4, CW04 (*DOB1*) and MS157-1A (*dob1-1*) after a 12 h shift to 37°C; lanes 5 and 6, JDY3 YCplac111-DOB1 (*DOB1*) and JDY3 pAS24-DOB1 (*GAL::DOB1*) were grown in YPGal and shifted to YPD for 36 h; lanes 7 and 8, D150 (*RRP4*) and P54 (*rrp4-1*) at 25°C; lane 9, P54 (*rrp4-1*) after a 12 h shift to 37°C; lanes 10 and 11, D150 (*RRP4*) and P79 (*GAL::RRP4*) were grown in YPGal and shifted to YPD for 36 h; lane 12, strain 966-1C (*Δxrn1 rat1-1*) at 23°C; lane 13, strain 966-1C (*Δxrn1 rat1-1*) after a 6 h shift to 37°C. RNA was extracted from exponentially growing cells. Equal amounts of total RNA were resolved on a 6% polyacrylamide–8 M urea gel and transferred to a Nylon membrane for Northern hybridization. (**A**) Hybridization with probe 2 (see Figure 1A for location of the probes), complementary to sequences within the 5′ ETS region. (**B**) Hybridization with probe 1, 3′ to site +1 in the 5′ ETS region. (**C**) Hybridization with probe 10, complementary to sequences within the 5′ ITS2 region. (**D**) Hybridization with probe 8, base pairing to sequences within the mature 5.8S rRNA species. The positions of the excised $5'-A_0$ fragment, 7S precursor and mature 5.8S rRNAs are indicated by horizontal arrows.

dob1-1 and *rrp4-1* mutations was substantially poorer than the growth of either single mutant strain at 25 or 30°C (Figure 9 and data not shown). Doubling times of 1.5, 2.6, 3.1 and 5.6 h were obtained for wild-type, *rrp4-1*, *dob1-1* and *dob1-1 rrp4-1* strains, respectively, grown at 30°C in YPD medium. However, a 2μ plasmid harbouring *RRP4* was unable to suppress the ts phenotype of the *dob1-1* mutation at 35 or 37°C (data not shown). No reciprocal suppression of the ts phenotype of the *rrp4-1* mutant was observed by a 2μ plasmid carrying *DOB1* (data not shown).

The similar phenotypes observed after mutation in, or *in vivo* depletion of, Dob1p or any component of the exosome, and the synthetic enhancement of the double *dob1-1 rrp4-1* mutant would be consistent with a physical interaction between Dob1p and the exosome complex. To
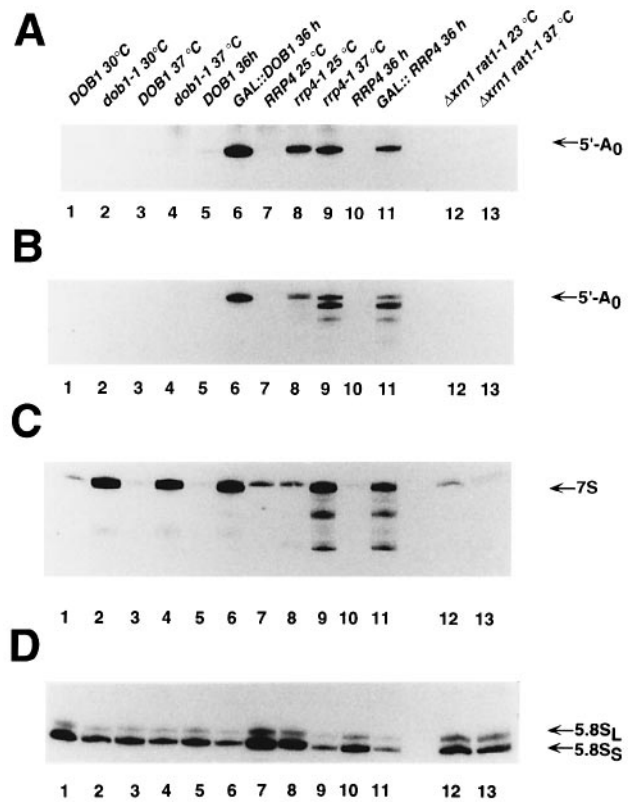
examine this hypothesis, a Prot-Rrp4p was immuno-precipitated from cell lysates of JDY7 (Table I) with IgG–agarose beads and immunoprecipitates were analysed by Western blot (see Materials and methods). More than 90% of total Prot-Rrp4p could be reproducibly precipitated; however, no co-immunoprecipitation of Dob1p was detected (data not shown).

We conclude that the putative RNA helicase Dob1p functionally interacts with the exosome complex both during the 3′ processing of 7S pre-rRNA and during the degradation of the excised $5'-A_0$ fragment. Dob1p does not, however, appear to be stably associated with the exosome complex.
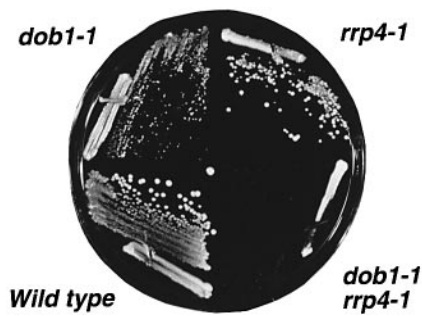
Fig. 9. Synthetic enhancement of the slow growth phenotype of the *dob1-1* mutant by *rrp4-1*. The strains MS157-1A (*dob1-1*), carrying the plasmid YCplac33-DOB1, and JDY4 (*rrp4-1*) were crossed and the resulting diploid sporulated. Complete tetrads were restreaked on 5-FOA-containing plates to counter-select YCplac33-DOB1. A representative tetratype tetrad after 5-FOA counter-selection is shown on a YPD plate. The plate was incubated for 4 days at 30°C.

Discussion

Here we have analysed the role of Dob1p, an essential putative ATP-dependent RNA helicase, in ribosome synthesis. Polysome analyses and quantification of total ribosomal subunits in the *dob1-1* and the *GAL::DOB1* strain revealed a deficit in 60S ribosomal subunits, leading to the appearance of half-mer polysomes. Similar profiles have been described for mutants defective in proteins of the 60S ribosomal subunits (Moritz *et al.*, 1991; Deshmukh *et al.*, 1993; Vilardell and Warner, 1997) and for mutants defective in components involved in pre-rRNA processing and 60S ribosomal subunit assembly (Ripmaster *et al.*, 1992; Hong *et al.*, 1997; Weaver *et al.*, 1997). Since we could not detect Dob1p in mature 60S ribosomal subunits, we concluded that Dob1p plays a role in the biogenesis of 60S ribosomal subunits. Consistent with this conclusion, pulse–chase analyses showed that the deficit in 60S ribosomal subunits in the *dob1-1* mutant is attributable to under-accumulation of the mature 25S and 5.8S rRNAs. In contrast, synthesis of the 18S and 5S rRNAs and methylation of pre-rRNAs were not affected by the *dob1-1* mutation. We have isolated the *dob1-1* mutation in a screen for dependence on overexpression of Tif3p. It recently has been postulated that mammalian eIF4B (the homologue of yeast Tif3p) serves as a bridge between the mRNA and the 40S ribosomal subunit, due to its ability to bind both mRNA and 18S rRNA, and interact with the p170 subunit of the 40S ribosomal subunit-associated factor eIF3 (Méthot *et al.*, 1996). Thus, ribosome binding could be facilitated by overexpression of Tif3p, partially bypassing the deficit in 60S ribosomal subunits in the *dob1-1* strain.

The most striking defect in *dob1-1* and *GAL::DOB1* strains is the strong accumulation of the 7S pre-rRNA, accompanied by reduced synthesis of the 5.8S rRNA. Since 25S and 5.8S rRNAs are both components of the 60S ribosomal subunit, reduced 5.8S rRNA synthesis is likely to account for the reduced accumulation of 25S rRNA seen by pulse–chase labelling in the *dob1-1* strain or, more severely, by Northern and primer extension analyses on RNA from the Dob1p-depleted strain. Processing of the 7S pre-rRNA to the 5.8S rRNA has been reported to be inhibited in strains that carry the *rrp4-1* mutation (Mitchell *et al.*, 1996) or which are genetically depleted of Rrp4p, Rrp41p, Rrp42p, Rrp43p or Rrp44p. These five proteins form a complex termed the exosome. Recombinant Rrp4p, Rrp41p and Rrp44p each have $3' \rightarrow 5'$ exonuclease activity, and Rrp42p and Rrp43p are each predicted to be $3' \rightarrow 5'$ exonucleases (Mitchell *et al.*, 1997). We conclude that the 7S pre-rRNA is processed to 5.8S rRNA by the $3' \rightarrow 5'$ exonuclease activity of the exosome, and that this also requires Dob1p, presumably acting as an RNA helicase.

Concomitant with the depletion of Dob1p, an excised fragment of the $5'$ ETS region also accumulates. This fragment extends from the $5'$ end of the 35S pre-rRNA to processing site A_0 (Figure 1A) and was designated $5'$-A_0. Strikingly, accumulation of the $5'$-A_0 fragment was also observed in strains carrying the *rrp4-1* mutation or genetically depleted of Rrp4p, Rrp41p, Rrp42p, Rrp43p or Rrp44p. From these observations, we conclude that pre-rRNA processing at site A_0 occurs by a direct endonucleolytic cleavage (see also Abou Elela *et al.*, 1996), and that the $5'$-A_0 fragment released is degraded $3' \rightarrow 5'$ by the exosome complex together with Dob1p.

In addition to the similarities of phenotypes observed in the Dob1p and exosome mutants, genetic data strongly support the close functional interaction between Dob1p and the exosome since the *dob1-1* mutation is synergistically enhanced by the *rrp4-1* mutation. We have, however, been unable to detect co-immunoprecipitation of Dob1p with Rrp4p. This does not exclude the possibility of a physical interaction between Dob1p and the exosome, but indicates that Dob1p is not stably associated with the complex.

The pre-RNA substrates (7S pre-rRNA and $5'$-A_0 fragment) are predicted to contain a high degree of secondary structure. The proposed structure of the $5'$-A_0 fragment includes nine major stable stem–loop structures of variable length and stability (Yeh and Lee, 1992), while the ITS2 region is predicted to fold into a compact cloverleaf-like structure containing four stable stem–loops (Yeh and Lee, 1990; van Nues *et al.*, 1995). Dob1p might facilitate the local unwinding of these RNA structures, allowing the exosome to associate with the pre-rRNA. Alternatively, Dob1p might open the RNA structure in front of the exosome preventing stalling of the complex. These possibilities are not, of course, mutually exclusive. In *E.coli*, a major pathway for mRNA decay involves the degradosome, a multi-component complex which contains the $3' \rightarrow 5'$ exoribonuclease PNPase and the endoribonuclease RNase E, together with the putative ATP-dependent RNA helicase RhlB (Py *et al.*, 1996). *In vitro*, the purified degradosome can completely degrade an RNA substrate containing a stem–loop element in the presence of ATP. In contrast, free PNPase, or the purified degradosome in the absence of ATP or after immunodepletion of RhlB, degrades this RNA only up to the stem–loop structure. These results suggested that RhlB acts by unwinding RNA secondary structures that impede the progression of the $3' \rightarrow 5'$ exonuclease activity of PNPase (Py *et al.*, 1996). A second example of an exoribonuclease-associated RNA helicase has come from the characterization of a $3' \rightarrow 5'$ exonuclease complex, termed the mtEXO, found in yeast mitochondria (Margossian *et al.*, 1996). The $3' \rightarrow 5'$ exonuclease activity of this complex probably resides in Dss1p, which is homologous to *E.coli* RNase II (Dmochowska *et al.*, 1995). Suv3p, a putative NTP-

dependent RNA helicase, is also a component of the mtEXO, and *suv3* mutants accumulate several excised fragments of group I introns (Margossian *et al.*, 1996).

In conclusion, we propose that Dob1p plays a broadly similar role to the putative RNA helicases associated with the degradosome and the mtEXO, but functions as a cofactor for the exosome rather than as an integral component of this complex. Dob1p is highly homologous to Ski2p, which is required for the $3' \rightarrow 5'$ exonucleolytic degradation of cytoplasmic mRNAs following poly(A) shortening. Moreover, this process also requires Rrp41p (Ski6p), a component of the exosome (J.Jacobs Anderson and R.Parker, in preparation). This suggests that Ski2p and Dob1p have similar functions as cofactors for the exosome in the cytoplasm and the nucleus, respectively.

During the course of this work, the *DOB1* gene was reported as *MTR4* (Liang *et al.*, 1996); mutations in *MTR4* lead to the nucleolar accumulation of poly(A)$^+$ RNA (Kadowaki *et al.*, 1994; Liang *et al.*, 1996). This accumulation has been attributed to a defect in nuclear–cytoplasmic transport of mRNA. In view of the role of Dob1p/Mtr4p in the $3' \rightarrow 5'$ processing and degradation of pre-rRNA, an alternative explanation would be that *mtr4* mutants are defective in a nuclear poly(A)$^+$ RNA turnover pathway. In this model, the role of Dob1p/Mtr4p would be analogous to the role of Ski2p in cytoplasmic mRNA degradation. It is notable that Dob1p is localized throughout the nucleus rather than only in the nucleolus (Liang *et al.*, 1996, and data not shown), indicating that it does have a nucleoplasmic function. No data are available on the level of nuclear RNA turnover in yeast, but in vertebrates a very substantial fraction of the nuclear RNA population (heterogeneous nuclear RNA) is degraded in the nucleus (Brandhorst and McConkey, 1974), indicating that such a turnover pathway must exist. Future experiments should allow us to provide evidence for whether Dob1p, acting in functional association with the exosome, also plays roles in the $3'$ end processing or degradation of other RNA substrates, including nuclear pre-mRNA.

Materials and methods

Strains, media and microbiological methods

The *S.cerevisiae* strains used in this study are listed in Table I. Most of them are isogenic to CW04, a derivative of W303 (Banroques *et al.*, 1986). Genetic manipulations and preparation of standard media were according to established procedures (Ausubel *et al.*, 1994; Kaiser *et al.*, 1994). Antibiotic-containing plates were prepared by adding the drugs from stock solutions into YPD before pouring the plates. Effective concentrations having no apparent effects on the growth of CW04 were 1 mg/ml paromomycin, 5 mg/ml neomycin and 0.1 μg/ml cycloheximide. Yeast cells were transformed using a lithium acetate method (Gietz *et al.*, 1992). *E.coli* DH10B was used for all recombinant DNA techniques (Sambrook *et al.*, 1989). Plasmid rescue from yeast into *E.coli* was performed as described (Ward, 1990).

Plasmids

Plasmid pDK17-TIF3 was constructed by cloning the *TIF3* gene as a 3.5 kb *Eco*RI fragment from pSEY18-STM1 (Coppolecchia *et al.*, 1993) into the *Eco*RI site of pASZ12-URA3. Plasmid pASZ12-URA3 was generated by introducing a 1.1 kb *Bgl*II *URA3* fragment from pFL44S (Bonneaud *et al.*, 1991) into the *Bam*HI site of the 2μ-*ADE2* plasmid pASZ12 (Stotz and Linder, 1990). YCplac111-TIF3 (*CEN-LEU2*), YEplac181-TIF3 (2μ-*LEU2*), YEplac181-CDC33, YEplac181-TIF2 and YEplac181-TIF4631 have been described (de la Cruz *et al.*, 1997). Plasmids pRS415-RRP4 (*CEN-LEU2*), pRS415-rrp4-1, pRS425-RRP4 (2μ-*LEU2*) and pRS416-ProtA-RRP4 (*CEN-URA3*) have been described previously (Mitchell *et al.*, 1996, 1997).

Isolation of TIF3 multicopy-dependent mutants

The strain MS04 was grown in YPD medium until mid-exponential phase, and five OD$_{600\,nm}$ units were resuspended in 1 ml of sterile 0.1 M sodium phosphate buffer, pH 7.0. Cells were treated with 30 μl of EMS (Sigma) for 50 min at 30°C, washed twice with 5 ml of a sterile 5% sodium thiosulfate solution, diluted in liquid YPD medium and plated out on YPD plates at a density of ~300 cells per plate. White, non-sectoring colonies were restreaked twice on YPD plates and tested for non-growth on plates containing 5-FOA. All plates were incubated at 30°C for 6 days.

Cloning and disruption of DOB1

The strain MS157-1A was transformed with a YCplac111-based yeast genomic library (D.Kressler, unpublished data), and transformants were selected on SD-Leu plates at 37°C. Eleven out of 30 000 Leu$^+$ transformants were able to restore wild-type growth. After plasmid rescue, only two overlapping clones (pDK102 and pDK103) were able to complement the ts phenotype reproducibly when back-transformed into MS157-1A. A 4 kb subclone from pDK102 was the minimal complementing fragment and was called YCplac111-DOB1. Plasmids YCplac33-DOB1, YEplac195-DOB1 and YEplac181-DOB1 were obtained by inserting a 4 kb *Kpn*I–*Sph*I fragment from YCplac111-DOB1 into the *Kpn*I–*Sph*I sites of YCplac33 (*CEN-URA3*), YEplac195 (2μ-*URA3*) and YEplac181 (2μ-*LEU2*) (Gietz and Sugino, 1988), respectively.

An almost complete *dob1* deletion construct was obtained by long flanking homology region-PCR (LFH-PCR) (Wach *et al.*, 1997). The oligonucleotide pairs MS157-5PL/MS157-P5 and MS157-3PL/MS157-P3 (Table II) were used for generating by PCR the 5′ LFH and 3′ LFH, respectively, using as a template genomic DNA from CW04. These PCR products were then used as primers to amplify the heterologous HIS3MX6 marker module from the *Eco*RV-linearized plasmid pFA6a-HIS3MX6 (Wach *et al.*, 1997). The final PCR products were used to transform the diploid ASZ3 strain. Five His$^+$ transformants were examined by Southern analysis to confirm that integration had occurred at the *DOB1* genomic locus. One disrupted strain, JDY1, was sporulated and tetrads were dissected. In addition, JDY1 was transformed with YCplac33-DOB1 and subjected to tetrad analysis. A His$^+$ haploid segregant (JDY3) that requires a plasmid-borne copy of *DOB1* for cell viability was used in further experiments.

Construction of a GAL::DOB1 allele and in vivo depletion of Dob1p

A 5 kb *Sph*I fragment from pDK103 containing the *DOB1* ORF was cloned into the *Sph*I site of a pUC19 vector lacking the *Kpn*I–*Bam*HI–*Xba*I restriction sites in its polylinker to generate pJC132. A 0.45 kb fragment, containing the 5′ end of the *DOB1* ORF, was PCR amplified using the oligonucleotides J7-MS157 and J9-MS157 (Table II), digested with *Sal*I and *Xba*I and cloned into those sites of pJC132 to generate plasmid pJC133. Finally, a 4 kb *Sal*I–*Sph*I fragment of pJC133 was cloned into the *Sal*I–*Sph*I sites of the YCplac111-based plasmid pAS24 (Schmidt *et al.*, 1997). The resulting plasmid, pAS24-DOB1, contains a *GAL1-10* promoter, a start codon followed by a double HA tag, and the *DOB1* ORF and its 3′ contiguous region. This construct was transformed into the strain JDY3 YCplac33-DOB1. The subsequent counter-selection of YCplac33-DOB1 on 5-FOA plates resulted in the strain JDY3 pAS24-DOB1. We also refer to this strain as *GAL::DOB1* or, if grown in YPD medium, as the Dob1p-depleted strain.

For *in vivo* depletion of Dob1p, JDY3 pAS24-DOB1 was grown in liquid medium containing galactose (YPGal) until mid-exponential phase. Cells were harvested, washed and resuspended in medium containing glucose (YPD). Cell growth was monitored over a period of 36 h, during which the cultures were diluted regularly into fresh YPD medium in order to maintain exponential growth. As a control, JDY3 YCplac111-DOB1 was used. Samples for Western blot, polysome analyses and RNA extraction were taken after 0, 6, 12, 24 and 36 h in YPD medium.

Pulse–chase labelling experiments

Pulse–chase labelling of pre-rRNA was performed as previously described (Sachs and Davis, 1990; Tollervey *et al.*, 1993) using 250 μCi of [methyl-^{3}H]methionine (Amersham, 70–85 Ci/mmol) or 50 μCi [5,6-^{3}H]uracil (Amersham, 45–50 Ci/mmol) per 40 OD$_{600\,nm}$ of yeast cells. Total RNA was extracted by the acid–phenol method (Ausubel *et al.*, 1994), and 20 000 c.p.m. ([methyl-^{3}H]methionine or [5,6-^{3}H]uracil labelling) were resolved on 1.2% agarose–formaldehyde gels (Venema *et al.*, 1997b). RNA was transferred to Hybond™-N$^+$ Nylon membranes (Amersham) by capillary blotting. After baking for 2 h at 80°C, the

Table II. Oligonucleotides used in this study

Name	Sequence (5′ to 3′)	Remarks
1[a]	CGAACGACAAGCCTACTCG	5′ ETS, 3′ to +1
2	GGTCTCTCTGCTGCCGG	5′ ETS, 5′ to A_0
3	CCAGATAACTATCTTAAAAG	5′ ETS, A_0/A_1/18S
4	CATGGCTTAATCTTTGAGAC	18S
5	GAAACGGTTTTAATTGTCCTATAAC	ITS1, D/A_2
6	TGTTACCTCTGGGCCC	ITS1, A_2/A_3
7	AATTTCCAGTTACGAAAATTCTTG	ITS1, A_3/B_1
8	TTTCGCTGCGTTCTTCATC	5.8S
9	TGAGAAGGAAATGACGCT	ITS2, E/C_2
10	GGCCAGCAATTTCAAGTTA	ITS2, E/C_2
11	GAACATTGTTCGCCTAGA	ITS2, $C_1/\bar{C}_2$
12	CTCCGCTTATTGATATGC	25S
13	GGTCACCCACTACACTACTCGG	5S
PX303	GAAGCGCCATCTAGATG	snR30
MS157-5PL	GGGGATCCGTCGACCTGCAGCGCATCCTTCGTATATAATCTATATTTCT	LFH-PCR disruption of *DOB1*
MS157-3PL	AAACGAGCTCGAATTCATCGATGATAGAGCTACTTTTACGCAAATCTGTAAA	LFH-PCR disruption of *DOB1*
MS157-P5	CGGGAAATTCTCGTCGGG	LFH-PCR disruption of *DOB1*
MS157-P3	TCTTGCAAAGTCCTTGTCCC	LFH-PCR disruption of *DOB1*
J4-MS157	GGGAATTCCATATGGATTCTACTG	PET22-NtDOB1
J5-MS157	CCGCTCGAGTTCGTCAACCACCAG	PET22-NtDOB1
J7-MS157	ACGCGTCGACGATTCTACTGATCTG	*GAL::DOB1*
J9-MS157	GTGCAACCTGGTGGCGGAC	*GAL::DOB1* and *HA-DOB1*
J11-MS157	CGGAATTCAGAGGAGCCAGTTCTGG	*HA-DOB1*
HA-DOB1-N5	AGGGATAGCCCGCATAGTCAGGAACATCGTATGGGTATGCCATCCTTCGTATATAATCTA	*HA-DOB1*
HA-DOB1-N3	TGACTATGCGGGCTATCCCTATGACGTCCCGGACTATGCACTCGAGGATTCTACTGATCTGTTCG	*HA-DOB1*

[a]For location of oligonucleotides 1–12, see Figure 1A.

membranes were sprayed with EN[3]HANCE™ (Du Pont), dried and exposed to X-ray films for 4 days at –80°C with an intensifying screen. For analysis of small RNAs, 20 000 c.p.m. ([5,6-^{3}H]uracil labelling) were resolved on 7% polyacrylamide–8 M urea gels. RNA was transferred to Hybond™-N[+] Nylon membranes as described (Venema *et al.*, 1997b), and the filters were baked and treated as described before.

Northern and primer extension analyses

Steady-state levels of mature and pre-rRNAs were assessed by Northern and primer extension analyses. The oligonucleotides 1–13 (Table II) were 5′ end-labelled with 30 μCi of [γ-^{32}P]ATP (Amersham, 5000 Ci/mmol) using T4 polynucleotide kinase (Appligene). Total RNA was extracted by the acid–phenol method (Ausubel *et al.*, 1994), and 5 μg were resolved on 1.2% agarose–formaldehyde or on 7% polyacrylamide–8 M urea gels. After transferring and immobilizing the RNA on Nylon membranes as above, the RNA was stained with 0.02% methylene blue in 0.3 M sodium acetate, pH 5.5. Pre-hybridization and hybridization were done in Church buffer (Church and Gilbert, 1984). Washes were done in 2× SSC, 0.5% SDS, and in 0.1× SSC, 0.5% SDS (Sambrook *et al.*, 1989). The membranes were then exposed to X-ray films at –80°C with an intensifying screen. Total RNA in Figure 8 was resolved on 6% polyacryamide–8 M urea gels, and the length of the 5′-A_0 species was estimated by comparing its apparent mobility with that of snR30, 7S pre-rRNA, 5.8S and 5S rRNAs.

Primer extension was performed as previously described (Venema *et al.*, 1997b) using as primers 5′ end ^{32}P-labelled oligonucleotides. To identify the positions of primer extension stops, DNA sequencing reactions were performed with the same oligonucleotides on rDNA-containing-plasmid templates.

Preparation of Dob1p antibodies

A recombinant N-terminal part of Dob1p was expressed in *E.coli* using a T7 system. To fuse the 5′ end of the *DOB1* ORF with the T7 promoter, a PCR was performed with the oligonucleotides J4-MS157 and J5-MS157, complementary to the 5′ end of the *DOB1* ORF and to the region +1017 to +1031, respectively. The primer J4-MS157 carries an additional *Nde*I site, in-frame with the first ATG in the *DOB1* ORF. The primer J5-MS157 carries an additional *Xho*I site. The ~1.1 kb PCR product was cut with *Nde*I–*Xho*I and cloned into pET22b(+) (Novagen). The resulting pET22b-NtDOB1 plasmid contains a His_6 tag sequence in-frame with the 3′ end of the cloned *DOB1* fragment. This plasmid was used to transform *E.coli* M0201 cells (Iost and Dreyfus, 1995), and two positive candidates were grown at 30°C in 500 ml of Luria broth medium containing 100 μg/ml ampicillin. At an $OD_{600\ nm}$ of 0.5,

production of T7 RNA polymerase was achieved by adding isopropyl-β-D-thiogalactopyranoside (IPTG) to a final concentration of 1 mM and the cultures were then shifted to 37°C. After 5 h, cells were harvested, washed with 50 mM sodium phosphate buffer, pH 8.0, containing 500 mM NaCl and resuspended in 5 ml of the same buffer. Then, cells were broken by ultrasonic treatment using a standard procedure (Sambrook *et al.*, 1989), and the extract was centrifuged at 8000 *g* for 5 min. The supernatant was mixed with 4 ml of Ni-NTA agarose (Qiagen) equilibrated in the above-mentioned buffer, and the recombinant protein was purified as described by the manufacturer. Approximately 5 mg of purified protein was dialysed against distilled water, lyophilized and resuspended in a phosphate-buffered saline solution for injection into two rabbits (Elevage Scientifique Des Dombes). Immune sera were used at a 1:5000 dilution.

Construction of a HA-Dob1 fusion protein and co-immunoprecipitations

To express an N-terminally HA-tagged Dob1 fusion protein from its own promoter, a fusion PCR was performed (Ho *et al.*, 1989). Briefly, two fragments with sequence overlap were generated in a first PCR series using *Eco*RI-restricted YCplac111-DOB1 as a template and the oligonucleotide couples J11-MS157/HA-DOB1-N3 and HA-DOB1-N5/J9-MS157. These PCR products, together with J11-MS157 and J9-MS157, were used for the final fusion PCR. The final product was cloned as an *Eco*RI–*Xba*I fragment into the *Eco*RI–*Xba*I sites of YCplac111-DOB1. This construct (YCplac111-HA-DOB1) was transformed into JDY3 YCplac33-DOB1, and then YCplac33-DOB1 was counter-selected on 5-FOA-containing plates. The strain JDY3 YCplac111-HA-DOB1 showed wild-type growth at all temperatures tested (18, 30 and 37°C). Quantitative Western blot analyses indicated that HA-Dob1p is expressed at wild-type levels.

For co-immunoprecipitations between Rrp4p and Dob1p, JDY3 YCplac111-HA-DOB1 and JDY5 (a ProtA-Rrp4p strain) were crossed to generate the diploid JDY6. JDY5 was obtained after transformation of P47 with pRS416-ProtA-RRP4 and subsequent tetrad dissection. The haploid strain JDY7, carrying the *rrp4* and *dob1* chromosomal deletions and complemented by the plasmids pRS416-ProtA-RRP4 and YCplac111-HA-DOB1, was obtained after tetrad dissection of JDY6. The strains JDY7 and JDY3 YCplac111-HA-DOB1 were grown in YPD at 30°C to an $OD_{600\ nm}$ of 0.8. Cells from 200 ml cultures were harvested and washed with cold water and cold lysis buffer (10 mM Tris–HCl, pH 7.5, 150 mM NaCl, 5 mM $MgCl_2$, and 0.1% NP-40). All subsequent steps, including cell breakage and immunoprecipitation, were performed as previously described (Mitchell *et al.*, 1996).

Miscellaneous

Cytoplasmic ribosome preparations, polysome analyses and quantification of total ribosomal subunits were performed according to Foiani *et al.* (1991) as previously described (de la Cruz *et al.*, 1997). Total yeast protein preparations were obtained by using a glass beads extraction method (Ausubel *et al.*, 1994). Immunoblotting was carried out according to standard procedures and decorated by the alkaline phosphatase procedure (Sambrook *et al.*, 1989). Preparations of yeast cells for immunofluorescence were done as described (Pringle *et al.*, 1991; Kressler *et al.*, 1997). For dideoxy sequencing, a T7 Sequencing™ kit (Pharmacia) was used. DNA and protein sequence comparisons were performed at the *Saccharomyces* Genome Database (Stanford) and at NCBI.

Acknowledgements

References

Abou Elela,S., Igel,H. and Ares,M.,Jr (1996) RNase III cleaves eukaryotic preribosomal RNA at a U3 snoRNP-dependent site. *Cell*, **85**, 115–124.

Altmann,M., Müller,P.P., Wittmer,B., Ruchti,F., Lanker,S. and Trachsel,H. (1993) A *Saccharomyces cerevisiae* homologue of mammalian translation initiation factor 4B contributes to RNA helicase activity. *EMBO J.*, **12**, 3997–4003.

Ausubel,F.M., Brent,R., Kingston,R.E., Moore,D.D., Seidman,J.G., Smith,J.A. and Struhl,K. (1994) *Saccharomyces cerevisiae*. In *Current Protocols in Molecular Biology*. John Wiley & Sons, Inc., pp. 13.0.1–13.14.17.

Banroques,J., Delahodde,A. and Jacq,C. (1986) A mitochondrial RNA maturase gene transferred to the yeast nucleus can control mitochondrial mRNA splicing. *Cell*, **46**, 837–844.

Bergès,T., Petfalski,E., Tollervey,D. and Hurt,E.C. (1994) Synthetic lethality with fibrillarin identifies NOP77p, a nucleolar protein required for pre-rRNA processing and modification. *EMBO J.*, **13**, 3136–3148.

Bonneaud,N., Ozier-Kalogeropoulos,O., Li,G., Labouesse,M., Minvielle-Sebastia,L. and Lacroute,F. (1991) A family of low and high copy replicative, integrative and single-stranded *S.cerevisiae/E.coli* shuttle vectors. *Yeast*, **7**, 609–615.

Brandhorst,B.P. and McConkey,E.H. (1974) Stability of nuclear RNA in mammalian cells. *J. Mol. Biol.*, **85**, 451–463.

Church,G.M. and Gilbert,W. (1984) Genomic sequencing. *Proc. Natl Acad. Sci. USA*, **81**, 1991–1995.

Coppolecchia,R., Buser,P., Stotz,A. and Linder,P. (1993) A new yeast translation initiation factor suppresses a mutation in the eIF-4A RNA helicase. *EMBO J.*, **12**, 4005–4011.

Dangel,A.W., Shen,L., Mendoza,A.R., Wu,L.-C. and Yu,C.Y. (1995) Human helicase gene *SKI2W* in the HLA class III region exhibits striking structural similarities to the yeast antiviral gene *SKI2* and to the human gene *KIAA0052*: emergence of a new gene family. *Nucleic Acids Res.*, **23**, 2120–2126.

de la Cruz,J., Iost,I., Kressler,D. and Linder,P. (1997) The p20 and Ded1 proteins have antagonistic roles in eIF4E-dependent translation in *Saccharomyces cerevisiae*. *Proc. Natl Acad. Sci. USA*, **94**, 5201–5206.

Deshmukh,M., Tsay,Y.-F., Paulovich,A.G. and Woolford,J.L.,Jr (1993) Yeast ribosomal protein L1 is required for the stability of newly synthesized 5S rRNA and the assembly of 60S ribosomal subunits. *Mol. Cell. Biol.*, **13**, 2835–2845.

Dmochowska,A., Golik,P. and Stepien,P.P. (1995) The novel nuclear *DSS1* of *Saccharomyces cerevisiae* is necessary for mitochondrial biogenesis. *Curr. Genet.*, **28**, 108–112.

Eichler,D.C. and Craig,N. (1994) Processing of eukaryotic ribosomal RNA. *Prog. Nucleic Acid Res. Mol. Biol.*, **49**, 197–239.

Foiani,M., Cigan,A.M., Paddon,C.J., Harashima,S. and Hinnebusch,A.G. (1991) GCD2, a translational repressor of the *GCN4* gene, has a general function in the initiation of protein synthesis in *Saccharomyces cerevisiae*. *Mol. Cell. Biol.*, **11**, 3203–3216.

Gietz,D., St. Jean,A., Woods,R.A. and Schiestl,R.H. (1992) Improved method for high efficiency transformation of intact yeast cells. *Nucleic Acids Res.*, **20**, 1425.

Gietz,R.D. and Sugino,A. (1988) New yeast–*Escherichia coli* shuttle vectors constructed with *in vitro* mutagenized yeast genes lacking six-base pair restriction sites. *Gene*, **74**, 527–534.

Henry,Y., Wood,H., Morrissey,J.P., Petfalski,E., Kearsey,S. and Tollervey,D. (1994) The 5′ end of yeast 5.8S rRNA is generated by exonucleases from an upstream cleavage site. *EMBO J.*, **13**, 2452–2463.

Ho,S.N., Hunt,H.D., Horton,R.M., Pullen,J.K. and Pease,L.R. (1989) Site-directed mutagenesis by overlap extension using the polymerase chain reaction. *Gene*, **77**, 51–59.

Hong,B., Brockenbrough,J.S., Wu,P. and Aris,J.P. (1997) Nop2p is required for pre-rRNA processing and 60S ribosome subunit synthesis in yeast. *Mol. Cell. Biol.*, **17**, 378–388.

Iost,I. and Dreyfus,M. (1995) The stability of *Escherichia coli* lacZ mRNA depends upon the simultaneity of its synthesis and translation. *EMBO J.*, **14**, 3252–3261.

Kadowaki,T., Chen,S., Hitomi,M., Jacobs,E., Kumagai,C., Liang,S., Schneiter,R., Wisniewska,J. and Tartakoff,A.M. (1994) Isolation and characterization of *Saccharomyces cerevisiae* mRNA transport-defective (*mtr*) mutants. *J. Cell Biol.*, **126**, 649–659.

Kaiser,C., Michaelis,S. and Mitchell,A. (1994) *Methods in Yeast Genetics: A Laboratory Course Manual*. Cold Spring Harbor Laboratory Press, Cold Spring Harbor, NY.

Kang,H.A. and Hershey,J.W. (1994) Effect of initiation factor eIF-5A depletion on protein synthesis and proliferation of *Saccharomyces cerevisiae*. *J. Biol. Chem.*, **269**, 3934–3940.

Kressler,D., de la Cruz,J., Rojo,M. and Linder,P. (1997) Fal1p is an essential DEAD-box protein involved in 40S-ribosomal-subunit biogenesis in *Saccharomyces cerevisiae*. *Mol. Cell. Biol.*, **17**, 7283–7294.

Lafontaine,D. and Tollervey,D. (1995) *Trans*-acting factors in yeast pre-rRNA and pre-snoRNA processing. *Biochem. Cell Biol.*, **73**, 803–812.

Liang,S., Hitomi,M., Hu,Y.-H., Liu,Y. and Tartakoff,A.M. (1996) A DEAD-box-family protein is required for nucleocytoplasmic transport of yeast mRNA. *Mol. Cell. Biol.*, **16**, 5139–5146.

Liang,W.-Q., Clark,J.A. and Fournier,M.J. (1997) The rRNA-processing function of the yeast U14 small nucleolar RNA can be rescued by a conserved RNA helicase-like protein. *Mol. Cell. Biol.*, **17**, 4124–4132.

Margossian,S.P., Li,H., Zassenhaus,H.P. and Butow,R.A. (1996) The DExH box protein Suv3p is a component of a yeast mitochondrial 3′-to-5′ exoribonuclease that suppresses group I intron toxicity. *Cell*, **84**, 199–209.

Mélèse,T. and Xue,Z. (1995) The nucleolus: an organelle formed by the act of building a ribosome. *Curr. Opin. Cell Biol.*, **7**, 319–324.

Méthot,N., Song,M.S. and Sonenberg,N. (1996) A region rich in aspartic acid, arginine, tyrosine, and glycine (DRYG) mediates eukaryotic initiation factor 4B (eIF4B) self-association and interaction with eIF3. *Mol. Cell. Biol.*, **16**, 5328–5334.

Mian,I.S. (1997) Comparative sequence analysis of ribonucleases HII, III, II, PH and D. *Nucleic Acids Res.*, **25**, 3187–3195.

Mitchell,P., Petfalski,E. and Tollervey,D. (1996) The 3′ end of yeast 5.8S rRNA is generated by an exonuclease processing mechanism. *Genes Dev.*, **10**, 502–513.

Mitchell,P., Petfalski,E., Shevchenko,A., Mann,M. and Tollervey,D. (1997) The exosome: a conserved eukaryotic RNA processing complex containing multiple 3′→5′ exoribonuclease activities. *Cell*, **91**, 457–466.

Moritz,M., Pulaski,B.A. and Woolford,J.L.,Jr (1991) Assembly of 60S ribosomal subunits is perturbed in temperature-sensitive yeast mutants defective in ribosomal protein L16. *Mol. Cell. Biol.*, **11**, 5681–5692.

O'Day,C.L., Chavanikamannil,F. and Abelson,J. (1996) 18S rRNA processing requires the RNA helicase-like protein Rrp3. *Nucleic Acids Res.*, **24**, 3201–3207.

Pringle,J.R., Adams,A.E.M., Drubin,D.G. and Haarer,B.K. (1991) Immunofluorescence methods for yeast. *Methods Enzymol.*, **194**, 565–602.

Py,B., Higgins,C.F., Krisch,H.M. and Carpousis,A.J. (1996) A DEAD-box RNA helicase in the *Escherichia coli* RNA degradosome. *Nature*, **381**, 169–172.

Ripmaster,T.L., Vaughn,G.P. and Woolford,J.L.,Jr (1992) A putative ATP-dependent RNA helicase involved in *Saccharomyces cerevisiae* ribosome assembly. *Proc. Natl Acad. Sci. USA*, **89**, 11131–11135.

Sachs,A.B. and Davis,R.W. (1990) Translation initiation and ribosomal biogenesis: involvement of a putative rRNA helicase and *RPL46*. *Science*, **247**, 1077–1079.

Sambrook,J., Fritsch,E.F. and Maniatis,T. (1989) *Molecular Cloning: A Laboratory Manual*. Cold Spring Harbor Laboratory Press, Cold Spring Harbor, NY.

Schmidt,A., Bickle,M., Beck,T. and Hall,M.N. (1997) The yeast phosphatidylinositol kinase homolog TOR2 activates RHO1 and RHO2 via the exchange factor ROM2. *Cell*, **88**, 531–542.

Stevens,A., Hsu,C.L., Isham,K.R. and Larimer,F.W. (1991) Fragments of the internal transcribed spacer 1 of pre-rRNA accumulate in *Saccharomyces cerevisiae* lacking 5′→3′ exoribonuclease 1. *J. Bacteriol.*, **173**, 7024–7028.

Stotz,A. and Linder,P. (1990) The *ADE2* gene from *Saccharomyces cerevisiae*: sequence and new vectors. *Gene*, **95**, 91–98.

Sun,C. and Woolford,J.L.,Jr (1994) The yeast *NOP4* gene product is an essential nucleolar protein required for pre-rRNA processing and accumulation of 60S ribosomal subunits. *EMBO J.*, **13**, 3127–3135.

Tollervey,D. and Kiss,T. (1997) Function and synthesis of small nucleolar RNAs. *Curr. Opin. Cell Biol.*, **9**, 337–342.

Tollervey,D., Lehtonen,H., Jansen,R., Kern,H. and Hurt,E.C. (1993) Temperature-sensitive mutations demonstrate roles for yeast fibrillarin in pre-rRNA processing, pre-rRNA methylation, and ribosome assembly. *Cell*, **72**, 443–457.

van Nues,R.W., Venema,J., Rientjes,J.M.J., Dirks-Mulder,A. and Raué,H.A. (1995) Processing of eukaryotic pre-rRNA: the role of the transcribed spacers. *Biochem. Cell Biol.*, **73**, 789–801.

Venema,J. and Tollervey,D. (1995) Processing of pre-ribosomal RNA in *Saccharomyces cerevisiae. Yeast*, **11**, 1629–1650.

Venema,J., Bousquet-Antonelli,C., Gelugne,J.-P., Caizergues-Ferrer,M. and Tollervey,D. (1997a) Rok1p is a putative RNA helicase required for rRNA processing. *Mol. Cell. Biol.*, **17**, 3398–3407.

Venema,J., Planta,R.J. and Raué,H.A. (1997b) *In vivo* mutational analysis of ribosomal RNA in *Saccharomyces cerevisiae*. In Martin,R. (ed.), *Protein Synthesis: Methods and Protocols*. Humana Press, Totowa, NJ, in press.

Vilardell,J. and Warner,J.R. (1997) Ribosomal protein L32 of *Saccharomyces cerevisiae* influences both the splicing of its own transcript and the processing of rRNA. *Mol. Cell. Biol.*, **17**, 1959–1965.

Wach,A., Brachat,A., Alberti-Segui,C., Rebischung,C. and Philippsen,P. (1997) Heterologous *HIS3* marker and GFP reporter modules for PCR-targeting in *Saccharomyces cerevisiae. Yeast*, **13**, 1065–1075.

Ward,A. (1990) Single-step purification of shuttle vectors from yeast for high frequency back-transformation into *E.coli. Nucleic Acids Res.*, **18**, 5319.

Weaver,P.L., Sun,C. and Chang,T.-H. (1997) Dbp3p, a putative RNA helicase in *Saccharomyces cerevisiae*, is required for efficient pre-rRNA processing predominantly at site A_3. *Mol. Cell. Biol.*, **17**, 1354–1365.

Widner,W.R. and Wickner,R.B. (1993) Evidence that the *SKI* antiviral system of *Saccharomyces cerevisiae* acts by blocking expression of viral mRNA. *Mol. Cell. Biol.*, **13**, 4331–4341.

Woolford,J.L.,Jr and Warner,J.R. (1991) The ribosome and its synthesis. In Broach,J.R., Pringle,J.R. and Jones,E.W. (eds), *The Molecular and Cellular Biology of the Yeast Saccharomyces. Genome Dynamics, Protein Synthesis and Energetics*. Cold Spring Harbor Laboratory Press, Cold Spring Harbor, NY, pp. 587–626.

Yeh,L.-C.C. and Lee,J.C. (1990) Structural analysis of the internal transcribed spacer 2 of the precursor ribosomal RNA from *Saccharomyces cerevisiae. J. Mol. Biol.*, **211**, 699–712.

Yeh,L.-C.C. and Lee,J.C. (1992) Structure analysis of the 5′ external transcribed spacer of the precursor ribosomal RNA from *Saccharomyces cerevisiae. J. Mol. Biol.*, **228**, 827–839.

Zanchin,N.I.T., Roberts,P., DeSilva,A., Sherman,F. and Goldfarb,D.S. (1997) *Saccharomyces cerevisiae* Nip7p is required for efficient 60S ribosome subunit biogenesis. *Mol. Cell. Biol.*, **17**, 5001–5015.